Sediment transport in Indian rivers high enough to impact satellite gravimetry

Alexandra Klemme[1], Thorsten Warneke[1], Heinrich Bovensmann[1], Matthias Weigelt[2], Jürgen Müller[2], Tim Rixen[3], Justus Notholt[1], and Claus Lämmerzahl[4]

[1]Institute of Environmental Physics, University of Bremen, Otto-Hahn-Allee 1, 28359 Bremen, Germany
[2]Institute of Geodesy, Leibniz Universität Hannover, Schneiderberg 50, 30167 Hannover, Germany
[3]Leibniz Center for Tropical Marine Research, Fahrenheitstr. 6, 28359 Bremen, Germany
[4]Centre of Applied Space Technology and Microgravity, University of Bremen, Am Fallturm 2, 28359 Bremen, Germany

Correspondence: A. Klemme (aklemme@uni-bremen.de)

Abstract. Satellite gravimetry is used to study the global hydrological cycle. It is a key component in the investigation of groundwater depletion on the Indian subcontinent. Terrestrial mass loss caused by river sediment transport is assumed to be below the detection limit in current gravimetric satellites of the Gravity Recovery and Climate Experiment Follow-On mission. Thus, it is not considered in the calculation of terrestrial water storage from such satellite data. However, the Ganges and Brahmaputra rivers, which drain the Indian subcontinent, constitute one of the world's most sediment rich river systems. In this study, we estimate the impact of sediment mass loss within their catchments on gravimetric estimates of trends in the local mass equivalent water height (EWH). We find that for the Ganges-Brahmaputra-Meghna catchment, sediment transport accounts for $(4 \pm 2)\%$ of the gravity decrease that is currently attributed to groundwater depletion. The sediment is mainly eroded from the Himalayas, where correction for the sediment mass loss reduces the decrease in EWH by $0.22\,\mathrm{cm\,yr^{-1}}$, which is about 14% of the EWH trend observed in that region. However, with sediment mass loss in the Brahmaputra catchment resulting to be more than twice that in the Ganges catchment and sediment mainly being eroded from mountain regions, the impact on gravimetric EWH data within the Indo-Gangetic plain, the main region identified for groundwater depletion, results to be comparatively small.

1 Introduction

Since March 2002, the Gravity recovery and Climate Experiment (GRACE) provides satellite based measurements of the Earth's gravity field (Dahle et al., 2019b), with the only major data gap being between the end of the original satellite mission in August 2017 and the launch of the follow-on mission (GRACE-FO) in May 2018. Gravity fields derived from satellite measurements yield information on global mass variations, which have proven crucial to monitor changes in global water storage and fluxes (Rodell et al., 2018). Retrieved data of the mass equivalent water height (EWH) are widely used for studies on e.g. glacier melting (Jacob et al., 2012; Luthcke et al., 2013), groundwater depletion (Rodell et al., 2009; Xie et al., 2020) and sea level rise (Cazenave et al., 2009; Jeon et al., 2018).

One significant region that yields a negative EWH trend is north-west India with an average decrease of $(29\pm2.5)\,\mathrm{m}^3\,\mathrm{H_2O}\,\mathrm{yr}^{-1}$ (Rodell et al., 2018; Xie et al., 2020). Several studies have investigated this decrease and explain it by a large-scale groundwater loss due to excessive extraction for irrigation (Tiwari et al., 2009; Rodell et al., 2009; Panda and Wahr, 2016; Rodell
25 et al., 2018; Xie et al., 2020). Wada et al. (2012) found that the use of non-renewable groundwater for irrigation more than trippled since 1960. In the year 2000, one-fifth of the global irrigation water demand was fed by non-renewable groundwater abstraction, with the majority being abstracted in India and Pakistan (Wada et al., 2012). Furthermore, the depletion in Indian groundwater occurred during a period of increased precipitation, implying an even stronger water deficit for future droughts (Rodell et al., 2018).

30 A large fraction of the Indian subcontinent is drained by the Ganges-Brahmaputra river system. The Ganges and Brahmaputra rivers originate in the Himalayan belt and drain intensely cultivated regions before their confluence in Bangladesh and discharge into the Bay of Bengal (Subramanian and Ramanathan, 1996; Garzanti et al., 2011). These rivers are one of the largest source of water and sediment to the world's ocean (Akter et al., 2021). The high amounts of sediment they carry into the Bay of Bengal make up the Bengal Delta and Submarine Fan that extends from Bangladesh to south of the equator and contains at
35 least $1.1\cdot10^{19}\,\mathrm{kg}$ of sediment with an average accumulation rate of $665\cdot10^{9}\,\mathrm{kg}\,\mathrm{yr}^{-1}$ (Curray, 1994). The sediment transport by the Ganges-Brahmaputra river system shows strong diurnal, seasonal and annual variations (Subramanian and Ramanathan, 1996) and estimates of sediment discharge vary widely between $200\cdot10^{9}\,\mathrm{kg}\,\mathrm{yr}^{-1}$ and $1{,}600\cdot10^{9}\,\mathrm{kg}\,\mathrm{yr}^{-1}$ for the Ganges River (Rahman et al., 2018; Holeman, 1968) and between $150\cdot10^{9}\,\mathrm{kg}\,\mathrm{yr}^{-1}$ and $1{,}157\cdot10^{9}\,\mathrm{kg}\,\mathrm{yr}^{-1}$ for the Brahmaputra River (Akter et al., 2021; Milliman and Meade, 1983). Yet, recent studies state the annual combined sediment discharge of the rivers to be
40 about $10^{12}\,\mathrm{kg}$ with the majority being carried during the monsoon season from June to October (Wasson, 2003; Kuehl et al., 2005; Wilson and Goodbred, 2015; Mouyen et al., 2018; Mahmud et al., 2020; Akter et al., 2021).

This river sediment transport implies a terrestrial mass reduction that has so far not been considered in the computation of gravimetric EWH data. A study by Schnitzer et al. (2013) found that the mass loss associated with the large-scale soil erosion in the Chinese Loess Plateau was not visible considering the available GRACE resolution. However, recent studies
45 found the sediment discharge to the ocean to be visible using satellite gravimetry of the estuary regions (Mouyen et al., 2018; Li et al., 2022). While the incorporation of sediment mass loss into monthly GRACE solutions over land might be impossible at the current satellite resolutions, it is a non-negligible loss when considering long term EWH trends studied in regard to e.g. groundwater depletion.

In this study, we estimate the impact of mass loss due to soil erosion and sediment transport by major rivers draining the
50 Indian subcontinent on EWH trends observed by the GRACE and GRACE-FO satellites.´

2 Methods

2.1 Study Area

This study focuses on the Ganges and Brahmaputra catchments, with some discussion of the Indus and Meghna catchments. The rivers are located mainly in Northern India but also partly flow through China, Pakistan, Nepal, Bhutan, Afghanistan and

Bangladesh (Figure 1). The river catchments are impacted by the South Asian monsoon, bringing high precipitation and river discharge from June to October, whereat the south-eastern parts of the catchments are effected earlier and longer than the north-western parts. The Ganges and Brahmaputra rivers originate in the Himalayan mountain belt and discharge into the Bay of Bengal after confluence with the Meghna river in Bangladesh. Together with the Indus River, they drain the majority of the Himalayas (Figure 1). Due to high erosion rates in the Himalayan mountain region, sediment concentrations in the rivers are among the highest worldwide (Subramanian and Ramanathan, 1996; Akter et al., 2021). More detailed river descriptions are included in the supplemental material.
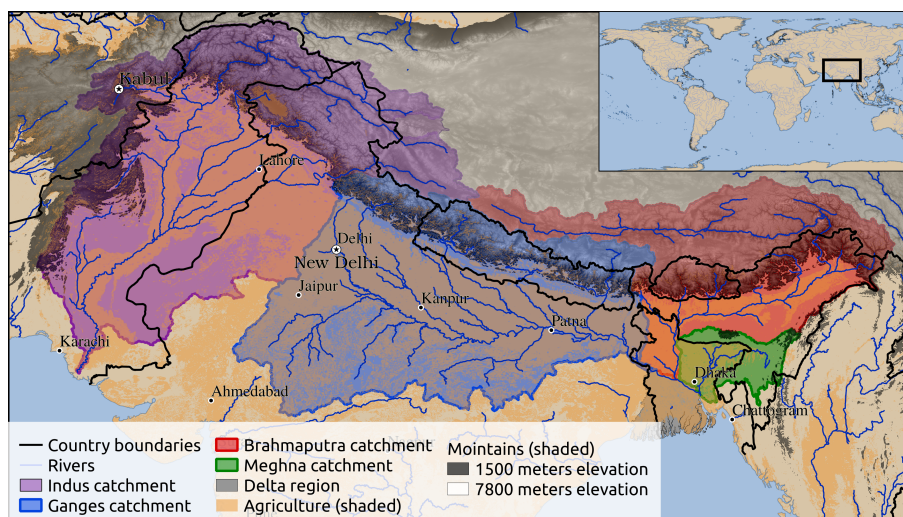
Figure 1. Map of investigated catchments and river paths as well as indicated areas of mountain (elevation $\geq 1500\,\mathrm{m}$) and agricultural regions. Elevation data is from Jarvis et al. (2008), agriculture regions are from GLCNMO (2017), river paths are from GRDC (2020) and river catchments are from Lehner and Grill (2013).

India hosts the world's largest groundwater-reliant agricultural irrigation system (Xie et al., 2020). Of its total irrigation-equipped area ($620,000\,\mathrm{km}^2$), about 64% can be irrigated with groundwater, amounting to a total consumptive groundwater use for irrigation of about $200\,\mathrm{km}^3\,\mathrm{yr}^{-1}$ (Siebert et al., 2010). The fraction of irrigation reliant on groundwater has increased over the past decades from only 29% in 1951 to more than 50% in 2022 (FAO, 2022), with the absolute groundwater irrigated area being more than 5 times larger than in 1951 (Siebert et al., 2010; FAO, 2022). The major groundwater aquifer for the studied regions is located in the Indo-Gangetic Plain and stretches mainly beneath the Indus and Ganges floodplains, while there are only shallow aquifers in the Himalayan mountain regions (Supplemental Figure S2).

This study specifically focuses on catchment fractions that are 1) utilized for agriculture or 2) located in erosion prone mountain regions of elevations $\geq 1,500\,\mathrm{m}$. The Ganges catchment includes 65.2% agricultural area and 15.9% mountain area (Table 1). The Brahmaputra catchment includes 18.2% agricultural area and 67.4% mountain area. In total, 36% of the studied region are located in the mountains and 39.3% are used for agriculture (Table 1).

Table 1. Mountain and agricultural fractions of the catchments.

	Total	GBM	Ganges	Brahmaputra	Meghna	Indus
catchment area (km^2)	2,679,070	1,576,135	950,754	539,989	58,391	864,452
mountain fraction (%)	36.0	32.9	15.9	67.4	3.3	51.6
agricultural fraction (%)	45.6	39.3	65.2	18.2	42.8	34.4

Total refers to the combined Ganges, Brahmaputra, Meghna and Indus catchments. GBM is the Ganges-Brahmaputra-Meghna catchment. Mountain fraction refers to regions of elevation $\geq 1,500\,m$ (based on elevation data from Jarvis et al., 2008). Agricultural regions are from GLCNMO (2017). River catchment data are from Lehner and Grill (2013).

2.2 Gravimetry and sediment data

Gravimetry data in this study is from the GRACE and GRACE-FO satellites. We use post-processed data from the Combination
75 International Service for Time-variable Gravity Fields (COST-G) Level 3 data product (Boergens et al., 2020) for terrestrial water storage anomalies in units of EWH. The data are based on the COST-G RL01 Level 2B products by Dahle and Murböck (2020) and include gridded data for EWH, EWH uncertainty, spatial leakage contained in the EWH and the background model atmospheric mass, all in a monthly resolution of $1° \times 1°$. The potential impact of filtering and spatial leakage in these data is discussed in the Supplemental Material.

80 Monthly EWH anomalies within the investigated catchments are derived by selecting all data whose grid centers are located within the respective catchment and calculating their area weighed average for each month. Data uncertainty is derived analogously from the area-weighed average of the EWH uncertainties provided in the COST-G data product. Linear least-squares optimizations of the generated monthly time-series yield the local EWH trends. Trend uncertainties contain the standard error of the derived slope optimization as well as the uncertainty of the monthly time series.

85 Sediment data for this study were collected from the literature. Generally, measurements in the study area are scarce and existing data is located close to Bangladesh, providing no information on the areal distribution of sediment loss in the upper catchments. The Supplemental Material provides a discussion on this scarcity in sediment data and the consequences for our study. Complete lists of the sediment data and their sources for the Ganges and Brahmaputra rivers are available in the supplemental tables S1 and S2, respectively.

90 ## 3 Results & Discussions

3.1 Geodetic observations of the decrease in equivalent water height

Gravimetric data of EWH generally show negative trends within the studied catchments. Trends are most pronounced in the eastern Brahmaputra catchment and in the western Ganges catchment at the border to the Indus catchment. The data yields the strongest decline of $5.8\,cm\,yr^{-1}$ in north-west India at about $28°N$ and $76°E$ (Figure 2).
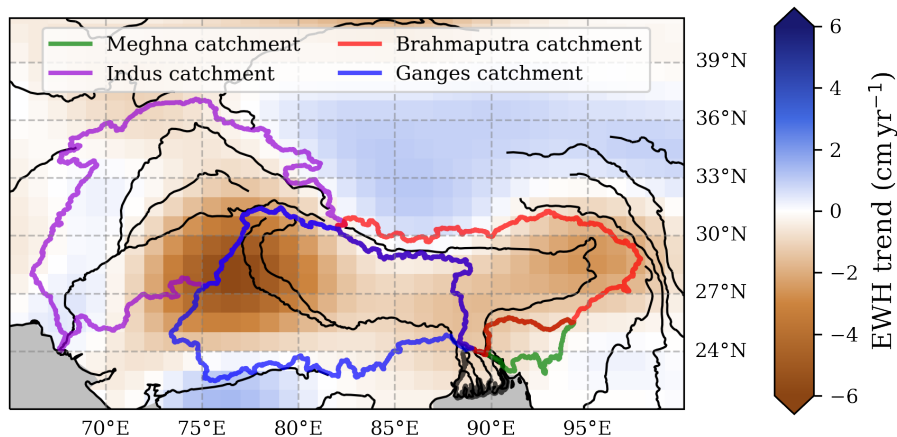
Figure 2. Trend of equivalent water height (EWH) with location of major river basins on the Indian subcontinent. Data were derived from linear least-squares approximation of the COST-G data (Boergens et al., 2020), based on the GRACE and GRACE-FO time period of 04-2002 to 12-2021. Location of river catchments are from Lehner and Grill (2013).

95   Comparison of average EWH trends within the individual catchments yields the strongest decrease for the Ganges catchment, followed by the Brahmaputra and Indus catchments. The Meghna catchment shows the weakest EWH decrease (Table 2). Low standard deviation of trends in the Brahmaputra and Meghna catchments imply rather homogeneous distributions of the EWH decrease in those catchments (Table 2). In the Ganges and Indus catchments, standard deviations are higher ($1.7 \, \mathrm{cm \, yr^{-1}}$ and $1.5 \, \mathrm{cm \, yr^{-1}}$ compared to $0.6 \, \mathrm{cm \, yr^{-1}}$ and $0.4 \, \mathrm{cm \, yr^{-1}}$) because the strong trends in those regions are caused by the
100 distinct negative trend in north-west India. This is confirmed further by the comparatively low median trend values within these catchments (Table 2).

Table 2. Loss of equivalent water height within the catchments.

EWH loss ($\mathrm{cm \, yr^{-1}}$)	Total	GBM	Ganges	Brahmaputra	Meghna	Indus	Ganges-m	Brahmaputra-m
mean	1.35	1.51	1.63	1.45	0.60	1.13	1.56	1.60
median	1.09	1.32	1.24	1.46	0.62	0.57	1.30	1.68
standard deviation	1.43	1.36	1.67	0.64	0.35	1.49	0.71	0.66
minimum	-1.12	-1.12	-1.12	0.27	0.09	-0.48	0.94	0.28
maximum	5.78	5.77	5.77	2.64	1.17	5.78	3.40	2.64

Data show the equivalent water height (EWH) loss. Accordingly, negative values represent a water height increase. GBM is the combined Ganges-Brahmaputra-Meghna catchment. Total refers to the combination of the Ganges, Brahmaputra, Meghna, and Indus catchmtens. Ganges-m and Brahmaputra-m refer to the mountain regions (altitude $\geq 1,500 \, \mathrm{m}$) within the Ganges and Brahmaputra catchment, respectively. Data was derived based on pixel-wise linear least-squares fit of the COST-G GACE data. The mean values are weighed by the different pixel areas while the other statistical variables do not consider respective pixel sizes.

Additional assessment of EWH trends in catchment mountain regions yields similar results for the Ganges and the Brahmaputra catchments ($1.6\,\mathrm{cm\,yr^{-1}}$, Table 2). For the Brahmaputra catchment, the observed EWH decrease is slightly higher than for the catchment average. For the Ganges catchment, it is slightly lower than the catchment average (Table 2). While the center

105 of the main EWH decrease in the Ganges catchment is located in the Indo-Gangetic plain, it extends into the Ganges mountain ranges. This implies that the EWH decrease in the Ganges mountain regions could be overestimated due to the impact of EWH leakage caused by data filtering, as discussed in the Supplemental Material.

For the combined study area, the average EWH decrease is $(1.4 \pm 0.2)\,\mathrm{cm\,yr^{-1}}$. The time series of EWH in the study area decreases fairly linear with annual variations, mainly driven by precipitation patterns that cause increasing EWH during the

110 monsoon months and decreasing EWH during dry periods (Figure 3, Supplemental Material). This EWH decrease over the complete study area of $2.68 \cdot 10^6\,\mathrm{km^2}$ represents a water mass reduction of $36 \cdot 10^{12}\,\mathrm{kg\,yr^{-1}}$ observed by gravimetry.
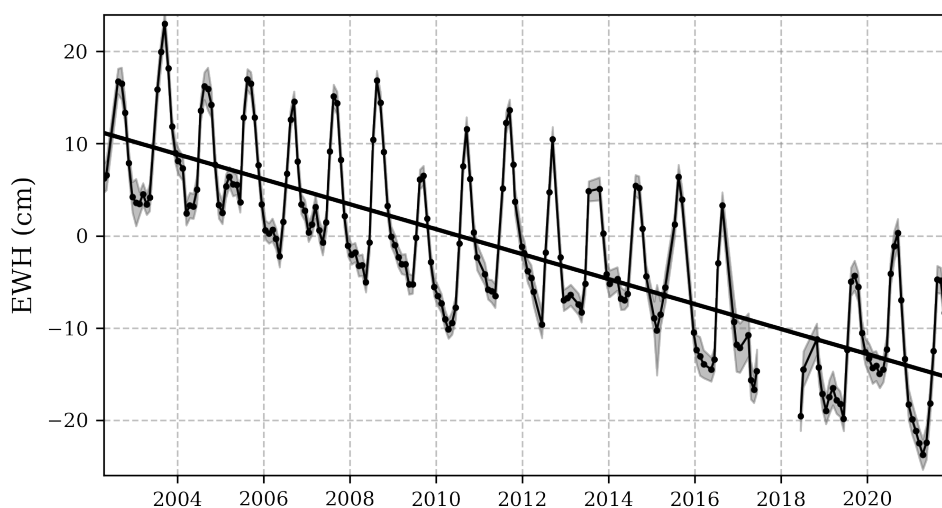
Figure 3. Time series of equivalent water height (EWH) within the total combined Ganges, Brahmaputra, Meghna and Indus catchments. Data points are area weighed monthly averages within the catchments and shaded areas represents area weighed uncertainties stated in the COST-G data product (Boergens et al., 2020). The linear trend was derived based on ordinary least-squares optimization of monthly data. The data gap represents the time between the end of the initial GRACE mission and the start of the GRACE-FO mission.

3.2 Mass loss caused by river sediment transport

To estimate the impact of sediment transport on the observed trend in gravity anomalies, we need the total sediment discharge from the studied regions. Based on data collected in various studies, the annual sediment discharge from the Ganges and

115 Brahmaputra rivers is $501 \cdot 10^9\,\mathrm{kg\,yr^{-1}}$ and $596 \cdot 10^9\,\mathrm{kg\,yr^{-1}}$, respectively. Sediment discharge from the Indus River is $168 \cdot 10^9\,\mathrm{kg\,yr^{-1}}$ and the Meghna River discharges $11 \cdot 10^9\,\mathrm{kg}$ of sediment per year (Table 3).

Table 3. River sediment transport within the catchments.

sediment load (10^9 kg yr^{-1})	Total	GBM	Ganges	Brahmaputra	Indus	Meghna
mean	1,276	2,008	501	596	168	11
median	1,207	1,082	480	590	125	12
standard deviation	633	511	272	237	122	2
minimum	400	350	200	150	50	0
maximum	3,147	2,777	1,600	1,157	370	20

Sediment loads are compiled from the literature. Total refers to the sum of sediment discharge in all four rivers. GBM refers
to sediment discharge in the Ganges-Brahmaputra-Meghna river system. The complete lists of data compiled for the Ganges
and Brahmaputra rivers are in the Supplemental Material in Table S1 and Table S2, respectively. Sediment load in the Meghna
River is compiled from Coleman (1969), Smith et al. (2009) and Rahman et al. (2018). Sediment load in the Indus River is
compiled from Holeman (1968), Milliman and Meade (1983), Giosan et al. (2006) and Mouyen et al. (2018).

Considering seasonality in sediment discharge based on water discharge stated in Islam (2016), more than 80% of the sediment is transported during the monsoon season from June to October (Supplemental Material). These periods of high sediment discharge correlate with the time of increasing EWH. Thus, the mass change due to sediment transport would reduce the gravimetric observations during EWH increase, while it has almost no impact on the observations during EWH decrease. In the following, however, we limit this study to an evaluation of the impact that annual sediment loss has on the gravimetric observations of the EWH decrease.

3.3 Impact of sediment transport on geodetic observations of trends in equivalent water height

3.3.1 Impact within the study area

To compare the mass loss from river sediment transport to the observed EWH trends, the absolute loss is divided by the respective catchment area and the density of water. This yields the absolute impact of sediment mass loss in units of EWH. The combined Indus, Ganges, Brahmaputra, and Meghna catchments cover an area of $2,679,070$ km^2 and experience a combined sediment mass loss of $1.3 \cdot 10^{12}$ kg yr^{-1}. This yields an absolute sediment mass impact of roughly 0.5 mm yr^{-1} in EWH that is not considered when deriving the EWH of terrestrial water storage based on gravimetric observations. This sediment mass loss needs to be subtracted from the observed EWH data, reducing the local EWH trend of 1.4 cm yr^{-1} by roughly 4% (Table 4).

This yields an average monthly sediment impact on EWH observations of less than 0.01 cm, which is well within the uncertainties stated for the GRACE EWH data within the study area (average EWH$_{\text{err}} \approx 1.4$ cm). However, considering the whole 20-year time-series, our results imply that about 1 cm of the observed EWH decrease currently attributed to groundwater depletion on the Indian subcontinent could be caused by sediment transport instead (Figure 4).

Exclusion of the Indus catchment yields a slightly stronger relative impact of sediment mass loss on the observed EWH trend for the Ganges-Brahmaputra-Meghna catchment. This can be explained by higher sediment discharge per catchment area (0.70 kg m^{-2} yr^{-1} compared to 0.48 kg m^{-2} yr^{-1}). The measured EWH decrease in the Ganges-Brahmaputra-Meghna

catchment, with is slightly higher than for the complete study area. Overall, our data yield an absolute sediment impact of $0.7 \, \mathrm{kg} \, \mathrm{m}^{-2} \, \mathrm{yr}^{-1}$. This implies that for the Ganges-Brahmaputra-Meghna catchment, about 4.6% of the observed gravity re-

140 duction currently attributed to groundwater loss could instead be caused by sediment transport. Over the total EWH data period, this would reduce the estimated EWH loss by $(1.6 \pm 0.8) \, \mathrm{cm}$ (supplemental Figure S7).
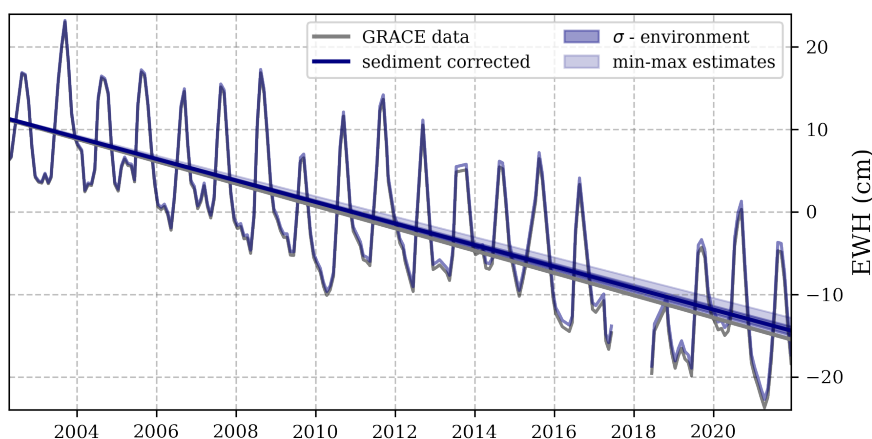
Figure 4. Time series of EWH derived from GRACE data and EWH corrected for sediment mass loss. Data are averaged over the combined Indus, Ganges, Brahmaputra, and Meghna catchments. Ranges for the σ-environment and the min-max estimates refet to the sediment estimates as stated in Table 3.

3.3.2 Impact within individual catchments

Investigation of the individual river catchments yields the highest sediment mass loss for the Brahmaputra catchment (Table 4), which is consistent with the high fraction of mountains in this catchment (Table 1) and the high precipitation rates that enhance

145 erosion in the Eastern Himalayas (Burbank et al., 2012). The absolute sediment mass loss in the Ganges catchment is similar to that in the Brahmaputra catchment. However, the Ganges catchment is larger than the Brahmaputra catchment, resulting in a sediment impact per catchment area that is only half that in the Brahmaputra catchment. Sediment mass loss in the Meghna and Indus catchments is significantly lower than in the Ganges and Brahmaputra catchment with only 0.13 and $0.15 \, \mathrm{kg} \, \mathrm{m}^{-2} \, \mathrm{yr}^{-1}$ compared to 1.10 and $0.53 \, \mathrm{kg} \, \mathrm{m}^{-2} \, \mathrm{yr}^{-1}$ (Table 4).

150 The observed reduction in GRACE EWH data is highest in the Ganges catchment and lowest in the Meghna catchment (Table 4). The fraction of the observed gravity anomalies potentially caused by sediment mass loss is highest for the Brahmaputra catchment at almost 8% (Table 4) that would reduce the groundwater attributed EWH decline for the whole data period by more than $2 \, \mathrm{cm}$ (Figure 5). The Indus and Meghna catchments show little impact of the sediment mass loss of 1.3% and 2.2%, respectively. In the Ganges catchment, sediment transport could be responsible for 3.3% of these gravity anomalies that are

155 currently attributed to groundwater loss.
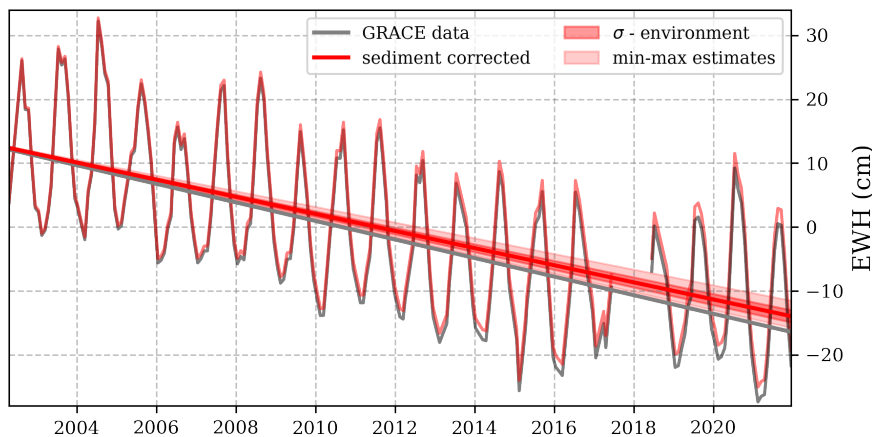
Figure 5. Time series of EWH derived from GRACE data and EWH corrected for sediment mass loss. Data show average over the whole Brahmaputra catchment. Ranges for the σ-environment and the min-max estimates refet to the sediment estimates as stated in Table 3. Analogue figures for the other catchments can be found in the supplemental figures S8, S9 and S10.

Table 4. Sediment impact on gravimetric observations of EWH trends for studied catchments.

river	catchment area (km^2)	sediment loss (10^{12} kg/yr)	GRACE EWH loss (mm/yr)	abs. sediment impact (kg/m^2/yr $\widehat{\approx}$ mm/yr)	rel. sediment impact (%)
Total	2,679,070	1.28 ± 0.63	13.5 ± 2.2	0.48 ± 0.23	3.6 ± 2.3
GBM	1,576,135	1.11 ± 0.51	15.1 ± 2.7	0.70 ± 0.32	4.6 ± 3.0
Ganges	950,754	0.50 ± 0.27	16.3 ± 2.8	0.53 ± 0.29	3.3 ± 2.3
Brahmaputra	539,989	0.60 ± 0.24	14.5 ± 2.6	1.10 ± 0.44	7.6 ± 4.4
Meghna	85,391	0.011 ± 0.002	6.0 ± 4.0	0.13 ± 0.02	2.2 ± 1.8
Indus	1,102,935	0.17 ± 0.12	11.3 ± 1.9	0.15 ± 0.11	1.3 ± 1.2
Ganges-m	148,948	$0.50 \pm 0.27^{(b)}$	15.6 ± 2.5	3.36 ± 1.83	21.5 ± 15.2
Ganges-HH	57,025	0.45 ± 0.27	$15.6 \pm 2.5^{(a)}$	7.89 ± 4.74	50.6 ± 38.6
Ganges-LH	91,885	0.05 ± 0.05	$15.6 \pm 2.5^{(a)}$	0.54 ± 0.54	3.5 ± 4.0
Brahmaputra-m	361,509	$0.60 \pm 0.24^{(b)}$	16.1 ± 2.3	1.65 ± 0.66	10.3 ± 5.6
Brahmaputra-ITS	21,600	0.27 ± 0.20	$16.1 \pm 2.3^{(a)}$	12.50 ± 9.26	77.6 ± 68.6
Brahmaputra-rem.	339,900	0.33 ± 0.22	$16.1 \pm 2.3^{(a)}$	0.97 ± 0.65	6.0 ± 4.9

Total refers to the combined Ganges, Brahmaputra, Meghna and Indus catchments. GBM is the Ganges-Brahmaputra-Meghna catchment. Ganges-m and Barhmaputra-m refer to the mountain regions (altitude $\geq 1,500$ m) within the Ganges and Brahmaputra catchment, respectively. Ganges-HH and Ganges-LH refer to the High Himalayas and the Lesser Himalayas in the Ganges catchment, respectively. Brahmaputra-ITS and Brahmaputra-rem. refer to the Indus-Tsangpo sutute and the remaining Brahmaputra mountains, respectively. $^{(a)}$EWH trends within specific locations in the catchment mountain regions are approximated by the average EWH trend over the mountains. $^{(b)}$Sediment data for the mountain regions assume all river sediment being eroded from these regions.

3.3.3 Impact within the Himalayan mountain regions

Studies agree that the majority of sediment discharged into the Bay of Bengal is derived from the Himalaya mountain ranges (Wasson, 2003; Galy et al., 2007; Faisal and Hayakawa, 2022). Thus, we specifically studied the impact of sediment mass loss in these regions.

160   The Brahmaputra catchment includes a mountain fraction of $67.4\,\%$ (Table 1). Assuming all of the river's sediment to be derived from these regions yields a sediment mass loss of $1.7\,\mathrm{kg\,m^{-2}\,yr^{-1}}$ (Table 4). The average EWH decrease derived from GRACE data for the region is $1.6\,\mathrm{cm\,yr^{-1}}$ (Table 4). Thus, assuming $100\,\%$ sediment origin within the Brahmaputra mountain regions, the sediment mass loss accounts to roughly $10\,\%$ of the EWH decrease currently attributed to groundwater reduction (Figure 6).

165   According to Faisal and Hayakawa (2022), about half $((45\pm15)\,\%)$ of the Brahmaputra's sediment is derived from the Indus-Tsangpo suture, a tectonic suture on the northern Himalayan margin that encompasses only $\approx 4\,\%$ of the Brahmaputra catchment. The remaining sediment is derived from Himalayan tributaries that join the Brahmaputra in the Himalayan foreland (Faisal and Hayakawa, 2022). This indicates a local sediment mass loss of $12.5\,\mathrm{kg\,m^{-2}\,yr^{-1}}$ within the Indus-Tsangpo suture and $1.0\,\mathrm{kg\,m^{-2}\,yr^{-1}}$ for the remaining Brahmaputra mountain areas. Such mass loss represents $78\,\%$ and $6\,\%$ of the observed
170   gravity anomaly in the Indus-Tsangpo suture and the remaining mountain regions, respectively (Table 4).
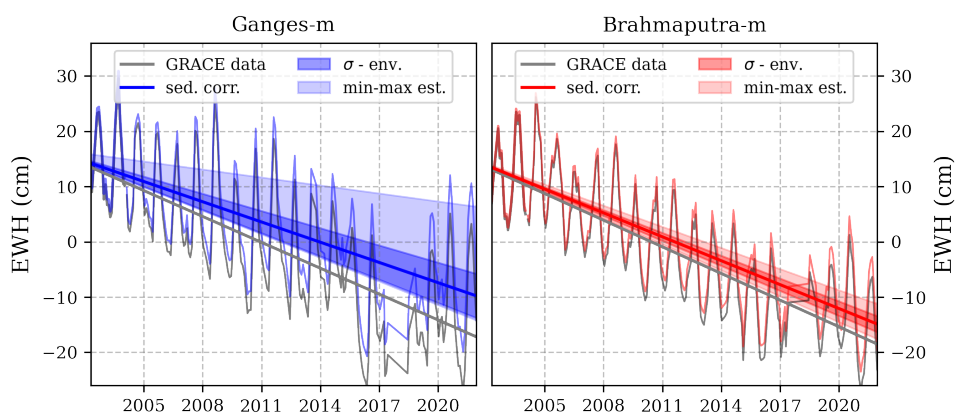
Figure 6. Time series of EWH derived from GRACE data and EWH after the correction for sediment mass loss. Data show average over the mountain fraction within the Ganges catchment (left) and the Brahmaputra catchment (right). σ environment and min-max estimates refer to the sediment discharge as stated in Table 3. An analogous figure for the mountain sub-regions is included in the supplement as Figure S11.

The Ganges catchment includes a mountain fraction of only $15.9\,\%$ (Table 1). Even though sediment discharge in the Ganges river is smaller, the area weighed mass loss over the mountains, with $3.4\,\mathrm{kg\,m^{-2}\,yr^{-1}}$, is about double that of the Brahmaputra mountains. Considering the slightly higher EWH decrease in the Ganges mountains, this sediment mass loss accounts for $22\,\%$ of the gravity anomaly observed in the area (Figure 6).

175   According to Faisal and Hayakawa (2022), $(90 \pm 5)\,\%$ of the Ganges sediment is derived from the High Himalayas. The remaining sediment is mostly from the Lesser Himalayas (Wasson, 2003) with a smaller contribution from intensely cultivated floodplain regions (Galy et al., 2007; Garzanti et al., 2011). Considering this, the local sediment loss from the High and Lesser Himalayas results to $7.9\,\mathrm{kg\,m^{-2}\,yr^{-1}}$ and $0.5\,\mathrm{kg\,m^{-2}\,yr^{-1}}$, respectively. For the High Himalayas, this represents about half the observed gravity anomaly, while for the Low Himalayas it is about $4\,\%$ (Table 4).

3.3.4   Impact on agricultural regions and observed groundwater depletion

Estimation of the sediment impact in river lowlands and floodplains is more complicated due to sedimentary redistribution within the catchments. While some sediment might be eroded in regions of excessive agriculture (Galy et al., 2007; Garzanti et al., 2011), there might also be regions of sediment storage and river accretion. Wasson (2003) estimated the fraction of Ganges sediment discharge that was eroded from floodplain regions to be $< 10\,\%$. Assuming this upper estimate of $10\,\%$ sediment being eroded from the location of the strongest observed GRACE EWH trend in southwest India (part of the Ganges catchment in $76\,°\mathrm{E}$ to $79\,°\mathrm{E}$ and $28\,°\mathrm{N}$ to $30\,°\mathrm{N}$), this represents a mass loss of roughly $0.9\,\mathrm{kg\,m^{-2}\,yr^{-1}}$ that could explain at most $2\,\%$ of the observed EWH decrease in this region ($5.4\,\mathrm{cm\,yr^{-1}}$).

    Assuming the floodplain sediment to be homogeneously eroded from the Ganges catchment located above the major aquifer in the Indo-Gangetic plain that is intensely cultivated with $88.7\,\%$ agricultural region (location of aquifer is in supplemental Figure S5), the average sediment mass loss is $(0.12 \pm 0.06)\,\mathrm{kg\,m^{-2}\,yr^{-1}}$, which represents less than $1\,\%$ of the observed gravity anomaly. Thus, despite high sediment discharge in these Indian rivers, the sediment mass loss impact on EWH trends in this main region of groundwater loss seems to be insignificant.

4   Conclusions

Our study shows the impact of sediment erosion on gravimetric estimates of terrestrial water loss within the main river catchments of the Indian subcontinent. Sediment erosion within the combined Ganges, Brahmaputra, Meghna, and Indus catchments yield an average mass loss of $(0.5 \pm 0.2)\,\mathrm{kg\,m^{-2}\,yr^{-1}}$ which potentially causes roughly $4\,\%$ of the EWH decrease currently attributed to groundwater loss. Exclusion of the Indus catchment increases the sediment impact to approximately $5\,\%$.

    Comparison of individual catchments yields, the highest impact of sediment mass loss is for the Brahmaputra catchment with $(1.1 \pm 0.4)\,\mathrm{kg\,m^{-2}\,yr^{-1}}$ that correspond to almost $8\,\%$ of the EWH decrease within this catchment. In the Ganges catchment, sediment transport represents $3.3\,\%$ of the EWH decrease, while for the Meghna and Indus catchment its $2.2\,\%$ and $1.3\,\%$, respectively.

    For mountain regions within the catchments, the regional sediment mass loss is even higher. Over the whole Ganges and Brahmaputra mountain ranges, we find sediment mass loss of $(2.2 \pm 1.0)\,\mathrm{kg\,m^{-2}\,yr^{-1}}$ with regional loss of $(3.4 \pm 1.8)\,\mathrm{kg\,m^{-2}\,yr^{-1}}$ in the Ganges mountains and $(1.7 \pm 0.7)\,\mathrm{kg\,m^{-2}\,yr^{-1}}$ in the Brahmaputra mountains. This represents $22\,\%$ and $10\,\%$ of the observed EWH loss in the Ganges and Brahmaputra mountains, respectively. Inspection of previously stated

erosion hotspots indicates that the sediment loss could potentially explain up to $77\,\%$ of the EWH decrease in selected mountain regions.

In the river floodplains, where gravimetric measurements show the strongest decrease, the sediment impact is smaller. The strongest EWH trend is observed in northwest India with a reduction of up to $5.8\,\mathrm{cm\,yr^{-1}}$. In this area, we find the sediment
210   mass loss to be at most $2\,\%$ with less than $1\,\%$ over the whole floodplain area.

Author contributions.   AK and TW developed the concept of the study. AK performed the analysis and led the writing of the paper. MW and JM contributed to the interpretation of geodetic data. TR helped interpret the sediment data. HB, JN and CL contributed to the general data interpretation. All authors discussed results and commented on the manuscript.

Competing interests.   The authors declare no competing interests.

References

Akter, J., Roelvink, D., and van der Wegen, M.: Process-based modeling deriving a long-term sediment budget for the Ganges-Brahmaputra-Meghna Delta, Bangladesh, Estuarine, Coastal and Shelf Science, 260, 107 509, https://doi.org/10.1016/j.ecss.2021.107509, 2021.

Boergens, E., Dobslaw, H., and Dill, R.: COST-G GravIS RL01 Continental Water Storage Anomalies. V. 0004., GFZ Data Services., https://doi.org/10.5880/COST-G.GRAVIS_01_L3_TWS, accessed 20.12.2022, 2020.

Burbank, D. W., Bookhagen, B., Gabet, E. J., and Putkonen, J.: Modern climate and erosion in the Himalaya, Comptes Rendus Geoscience, 344, 610–626, https://doi.org/10.1016/j.crte.2012.10.010, erosion–Alteration: from fundamental mechanisms to geodynamic consequences (Ebelmen's Symposium), 2012.

Cazenave, A., Dominh, K., Guinehut, S., Berthier, E., Llovel, W., Ramillien, G., Ablain, M., and Larnicol, G.: Sea level budget over 2003–2008: A reevaluation from GRACE space gravimetry, satellite altimetry and Argo, Global and Planetary Change, 65, 83–88, https://doi.org/10.1016/j.gloplacha.2008.10.004, 2009.

Coleman, J. M.: Brahmaputra river: Channel processes and sedimentation, Sedimentary Geology, 3, 129–239, https://doi.org/10.1016/0037-0738(69)90010-4, brahmaputra river: Channel processes and sedimentation, 1969.

Curray, J. R.: Sediment volume and mass beneath the Bay of Bengal, Earth and Planetary Science Letters, 125, 371–383, https://doi.org/10.1016/0012-821X(94)90227-5, 1994.

Dahle, C. and Murböck, M.: Post-processed GRACE/GRACE-FO Geopotential GSM Coefficients COST-G RL01 (Level-2B Product). V. 0002., GFZ Data Services., https://doi.org/https://doi.org/10.5880/COST-G.GRAVIS_01_L2B, 2020.

Dahle, C., Flechtner, F., Murböck, M., Michalak, G., Neumayer, K. H., Abrykosov, O., Reinhold, A., and König, R.: GRACE-FO Geopotential GSM Coefficients GFZ RL06. V. 6.0., GFZ Data Services., https://doi.org/10.5880/GFZ.GRACEFO_06_GSM, accessed 10.5.2022, 2019a.

Dahle, C., Murböck, M., Flechtner, F., Dobslaw, H., Michalak, G., Neumayer, K. H., Abrykosov, O., Reinhold, A., König, R., Sulzbach, R., and Förste, C.: The GFZ GRACE RL06 Monthly Gravity Field Time Series: Processing Details and Quality Assessment, Remote Sensing, 11, https://doi.org/10.3390/rs11182116, 2019b.

Faisal, B. M. R. and Hayakawa, Y. S.: Geomorphological processes and their connectivity in hillslope, fluvial, and coastal areas in Bangladesh: A review, Progress in Earth and Planetary Science, 9, https://doi.org/10.1186/s40645-022-00500-8, 2022.

FAO: AQUASTAT Core Database., Food and Agriculture Organization of the United Nations., accessed via https://tableau.apps.fao.org/views/ReviewDashboard-v1/country_dashboard?%3Aembed=y&%3AisGuestRedirectFromVizportal=y (17.11.2022), 2022.

Galy, V., France-Lanord, C., Beyssac, O., Faure, P., Kudrass, H., and Palhol, F.: Efficient organic carbon burial in the Bengal fan sustained by the Himalayan erosional system, Nature, 450, https://doi.org/10.1038/nature06273, 2007.

Garzanti, E., Andó, S., France-Lanord, C., Censi, P., Vignola, P., Galy, V., and Lupker, M.: Mineralogical and chemical variability of fluvial sediments 2. Suspended-load silt (Ganga–Brahmaputra, Bangladesh), Earth and Planetary Science Letters, 302, 107–120, https://doi.org/10.1016/j.epsl.2010.11.043, 2011.

Giosan, L., Constantinescu, S., Clift, P. D., Tabrez, A. R., Danish, M., and Inam, A.: Recent morphodynamics of the Indus delta shore and shelf, Continental Shelf Research, 26, 1668–1684, https://doi.org/10.1016/j.csr.2006.05.009, 2006.

GLCNMO: Global Land Cover by National Mapping Organizations: GLCNMO Version 3, Geospatial Information Authority of Japan, Chiba University and Collaborating Organizations, accessed via https://github.com/globalmaps/gm_lc_v3 (26.10.2022), 2017.

GRDC: Major River Basins of the World: "Major Rivers", Global Runoff Data Centre. 2nd, rev. ext. ed. Koblenz, Germany: Federal Institute of Hydrology (BfG), accessed via: https://www.bafg.de/SharedDocs/ExterneLinks/GRDC/mrb_shp_zip.html;jsessionid= 993792470F4B2723B3942ACFA8C09C66.live11313?nn=201762 (24.10.2022)., 2020.

Holeman, J. N.: The Sediment Yield of Major Rivers of the World, Water Resources Research, 4, 737–747,
https://doi.org/10.1029/WR004i004p00737, 1968.

Islam, S.: Deltaic floodplains development and wetland ecosystems management in the Ganges–Brahmaputra–Meghna Rivers Delta in Bangladesh, Sustainable Water Resources Management, 2, https://doi.org/10.1007/s40899-016-0047-6, 2016.

Jacob, T., Wahr, J., Pfeffer, W. T., and Swenson, S.: Recent contributions of glaciers and ice caps to sea level rise., Nature, https://doi.org/10.1038/nature10847, 2012.

Jarvis, A., Reuter, H., Nelson, A., and Guevara, E.: Hole-filled seamless SRTM data V4, International Centre for Tropical Agriculture (CIAT), accessed from https://srtm.csi.cgiar.org (24.10.2022)., 2008.

Jeon, T., Seo, K.-W., Youm, K., Chen, J., and Wilson, C. R.: Global sea level change signatures observed by GRACE satellite gravimetry, Scientific Reports, 8, https://doi.org/10.1038/s41598-018-31972-8, 2018.

Kuehl, S. A., Allison, M. A., Goodbred, S. L., and Kudrass, H.: The Ganges-Brahmaputra Delta, in: River Deltas–Concepts, Models, and Examples, SEPM Society for Sedimentary Geology, https://doi.org/10.2110/pec.05.83.0413, 2005.

Lehner, B. and Grill, G.: Global river hydrography and network routing: baseline data and new approaches to study the world's large river systems., https://doi.org/10.1002/hyp.9740, accessed via https://www.hydrosheds.org/products/hydrobasins (20.10.2022), 2013.

Li, Z., Zhang, Z., Scanlon, B. R., Sun, A. Y., Pan, Y., Qiao, S., Wang, H., and Jia, Q.: Combining GRACE and satellite altimetry data to detect change in sediment load to the Bohai Sea, Science of The Total Environment, 818, 151 677, https://doi.org/10.1016/j.scitotenv.2021.151677, 2022.

Luthcke, S. B., Sabaka, T., Loomis, B., Arendt, A., McCarthy, J., and Camp, J.: Antarctica, Greenland and Gulf of Alaska land-ice evolution from an iterated GRACE global mascon solution, Journal of Glaciology, 59, 613–631, https://doi.org/10.3189/2013JoG12J147, 2013.

Mahmud, M. I., Mia, A. J., Islam, M. A., Peas, M. H., Farazi, A. H., and Akhter, S. H.: Assessing bank dynamics of the Lower Meghna River in Bangladesh: an integrated GIS-DSAS approach, Arabian Journal of Geosciences, 13, https://doi.org/10.1007/s12517-020-05514-4, 2020.

Milliman, J. D. and Meade, R. H.: World-Wide Delivery of River Sediment to the Oceans, The Journal of Geology, 91, 1–21, http://www.jstor.org/stable/30060512, 1983.

Milliman, J. D. and Syvitski, J. P. M.: Geomorphic/Tectonic Control of Sediment Discharge to the Ocean: The Importance of Small Mountainous Rivers, The Journal of Geology, 100, 525–544, https://doi.org/10.1086/629606, 1992.

Mouyen, M., Longuevergne, L., Steer, P., Crave, A., Lemoine, J.-M., Save, H., and Robin, C.: Assessing modern river sediment discharge to the ocean using satellite gravimetry, Nature Communications, 9, https://doi.org/10.1038/s41467-018-05921-y, 2018.

Panda, D. K. and Wahr, J.: Spatiotemporal evolution of water storage changes in India from the updated GRACE-derived gravity records, Water Resources Research, 52, 135–149, https://doi.org/10.1002/2015WR017797, 2016.

Rahman, M., Dustegir, M., Karim, R., Haque, A., Nicholls, R. J., Darby, S. E., Nakagawa, H., Hossain, M., Dunn, F. E., and Akter, M.: Recent sediment flux to the Ganges-Brahmaputra-Meghna delta system, Science of The Total Environment, 643, 1054–1064, https://doi.org/10.1016/j.scitotenv.2018.06.147, 2018.

Rodell, M., Velicogna, I., and Famiglietti, J. S.: Satellite-based estimates of groundwater depletion in India, Nature, 460, https://doi.org/10.1038/nature08238, 2009.

Rodell, M., Famiglietti, J. S., Wiese, D. N., Reager, J. T., Beaudoing, H. K., Landerer, F. W., and Lo, M.-H.: Emerging trends in global
290   freshwater availability, Nature, 557, https://doi.org/10.1038/s41586-018-0123-1, 2018.

Schnitzer, S., Seitz, F., Eicker, A., Güntner, A., Wattenbach, M., and Menzel, A.: Estimation of soil loss by water erosion in
the Chinese Loess Plateau using Universal Soil Loss Equation and GRACE, Geophysical Journal International, 193, 1283–1290,
https://doi.org/10.1093/gji/ggt023, 2013.

Siebert, S., Burke, J., Faures, J. M., Frenken, K., Hoogeveen, J., Döll, P., and Portmann, F. T.: Groundwater use for irrigation – a global
295   inventory, Hydrology and Earth System Sciences, 14, 1863–1880, https://doi.org/10.5194/hess-14-1863-2010, 2010.

Smith, G. S., Best, J. L., Bristow, C. S., and Petts, G. E.: Braided Rivers: process, deposits, ecology and management., https://www.wiley.
com/en-us/Braided+Rivers:+Process,+Deposits,+Ecology+and+Management-p-9781444304374, 2009.

Subramanian, V. and Ramanathan, A. L.: Nature of Sediment Load in the Ganges-Brahmaputra River Systems in India, pp. 151–168, Springer
Netherlands, Dordrecht, https://doi.org/10.1007/978-94-015-8719-8_8, 1996.

300   Tiwari, V. M., Wahr, J., and Swenson, S.: Dwindling groundwater resources in northern India, from satellite gravity observations, Geophysical
Research Letters, 36, https://doi.org/https://doi.org/10.1029/2009GL039401, 2009.

Wada, Y., van Beek, L. P. H., and Bierkens, M. F. P.: Nonsustainable groundwater sustaining irrigation: A global assessment, Water Resources
Research, 48, https://doi.org/10.1029/2011WR010562, 2012.

Wasson, R. J.: A sediment budget for the Ganga–Brahmaputra catchment, Current Science, 84, 1041–1047, http://www.jstor.org/stable/
305   24107666, 2003.

Wilson, C. A. and Goodbred, S. L.: Construction and Maintenance of the Ganges-Brahmaputra-Meghna Delta: Linking Process, Morphology,
and Stratigraphy, Annual Review of Marine Science, 7, 67–88, https://doi.org/10.1146/annurev-marine-010213-135032, pMID: 25251271,
2015.

Xie, H., Longuevergne, L., Ringler, C., and Scanlon, B.: Integrating groundwater irrigation into hydrological simulation of India: Case of
310   improving model representation of anthropogenic water use impact using GRACE, Journal of Hydrology: Regional Studies, 29, 100 681,
https://doi.org/10.1016/j.ejrh.2020.100681, 2020.